

# Lawrence Berkeley National Laboratory

## LBL Publications

### Title

$\{\xi\}\{\omega\}$  Production in Pb+Pb Collisions at 158 GeV/c

### Permalink

<https://escholarship.org/uc/item/5zr5x9mw>

### Author

Odyniec, G.

### Publication Date

1997-06-13

# $\Xi$ ( $\Omega$ ) Production in Pb+Pb Collisions at 158 GeV/c

G.Odyniec<sup>2</sup> for the NA49 Collaboration

S.V. Afanasiev<sup>9</sup>, T. Alber<sup>13</sup>, H. Appelshäuser<sup>7</sup>, J. Bächler<sup>5</sup>, S.J. Bailey<sup>16</sup>,  
L.S. Barnby<sup>3</sup>, J. Bartke<sup>6</sup>, H. Bialkowska<sup>14</sup>, C.O. Blyth<sup>3</sup>, R. Bock<sup>7</sup>,  
C. Bormann<sup>10</sup>, F.P. Brady<sup>8</sup>, R. Brockmann<sup>7</sup>, N. Buncic<sup>5,10</sup>,  
P. Buncic<sup>5,10</sup>, H.L. Caines<sup>3</sup>, D. Cebra<sup>8</sup>, P. Chan<sup>16</sup>, G.E. Cooper<sup>2</sup>,  
J.G. Cramer<sup>16,13</sup>, P.B. Cramer<sup>16</sup>, P. Csato<sup>4</sup>, O. Dietz<sup>10</sup>, J. Dunn<sup>8</sup>,  
V. Eckardt<sup>13</sup>, F. Eckhardt<sup>12</sup>, M.I. Ferguson<sup>5</sup>, H.G. Fischer<sup>5</sup>, D. Flierl<sup>10</sup>,  
Z. Fodor<sup>4</sup>, P. Foka<sup>7,10</sup>, P. Freund<sup>13</sup>, V. Friese<sup>12</sup>, M. Fuchs<sup>10</sup>, F. Gabler<sup>10</sup>,  
J. Gal<sup>4</sup>, M. Gaździcki<sup>10</sup>, E. Gładysz<sup>6</sup>, J. Grebieszko<sup>15</sup>, J. Günther<sup>10</sup>,  
J.W. Harris<sup>17</sup>, S. Hegyi<sup>4</sup>, T. Henkel<sup>12</sup>, L.A. Hill<sup>3</sup>, I. Huang<sup>2,8</sup>,  
M.A. Howe<sup>16</sup>, H. Hümmeler<sup>10</sup>, G. Igo<sup>11</sup>, D. Irmscher<sup>2,7,+</sup>, P. Jacobs<sup>2</sup>,  
P.G. Jones<sup>3</sup>, K. Kadija<sup>18,13</sup>, V.I. Kolesnikov<sup>9</sup>, A. Konashenok<sup>2</sup>,  
M. Kowalski<sup>6</sup>, B. Lasiuk<sup>11</sup>, P. Lévai<sup>4</sup>, A.I. Malakhov<sup>9</sup>, S. Margetis<sup>2,8</sup>,  
C. Markert<sup>7</sup>, G.L. Melkumov<sup>9</sup>, A. Mock<sup>13</sup>, J. Molnár<sup>4</sup>, J.M. Nelson<sup>3</sup>,  
G. Odyniec<sup>2</sup>, G. Palla<sup>4</sup>, A.D. Panagiotou<sup>1</sup>, A. Petridis<sup>1</sup>, A. Piper<sup>12</sup>,  
R.J. Porter<sup>2</sup>, A.M. Poskanzer<sup>2,\*</sup>, S. Poziombka<sup>10</sup>, D.J. Prindle<sup>16</sup>,  
F. Pühlhofer<sup>12</sup>, W. Rauch<sup>13</sup>, J.G. Reid<sup>16</sup>, R. Renfordt<sup>10</sup>, W. Retyk<sup>15</sup>,  
H.G. Ritter<sup>2</sup>, D. Röhrich<sup>10</sup>, C. Roland<sup>7</sup>, G. Roland<sup>10</sup>, H. Rudolph<sup>2,10</sup>,  
A. Rybicki<sup>6</sup>, I. Sakrejda<sup>2</sup>, A. Sandoval<sup>7</sup>, H. Sann<sup>7</sup>, A.Yu. Semenov<sup>9</sup>,  
E. Schäfer<sup>13</sup>, D. Schmischke<sup>10</sup>, N. Schmitz<sup>13</sup>, S. Schönfelder<sup>13</sup>,  
P. Seyboth<sup>13</sup>, J. Seyerlein<sup>13</sup>, F. Sikler<sup>4</sup>, E. Skrzypczak<sup>15</sup>, G.T.A. Squier<sup>3</sup>,  
R. Stock<sup>10</sup>, H. Ströbele<sup>10</sup>, I. Szentpetery<sup>4</sup>, J. Sziklai<sup>4</sup>, M. Toy<sup>2,11</sup>,  
T.A. Trainor<sup>16</sup>, S. Trentalange<sup>11</sup>, T. Ullrich<sup>17</sup>, M. Vassiliou<sup>1</sup>,  
G. Vesztegombi<sup>4</sup>, D. Vranic<sup>7,18</sup>, F. Wang<sup>2</sup>, D.D. Weerasundara<sup>16</sup>,  
S. Wenig<sup>5</sup>, C. Whitten<sup>11</sup>, T. Wienold<sup>2,+,#</sup>, L. Wood<sup>8</sup>, T.A. Yates<sup>3</sup>,  
J. Zimanyi<sup>4</sup>, X.-Z. Zhu<sup>16</sup>, R. Zybert<sup>3</sup>

<sup>1</sup>Department of Physics, University of Athens, Athens, Greece, <sup>2</sup>Lawrence Berkeley National Laboratory, University of California, Berkeley, USA, <sup>3</sup>Birmingham University, Birmingham, England, <sup>4</sup>KFKI Research Institute for Particle and Nuclear Physics, Budapest, Hungary, <sup>5</sup>CERN, Geneva, Switzerland, <sup>6</sup>Institute of Nuclear Physics, Cracow, Poland, <sup>7</sup>Gesellschaft für Schwerionenforschung (GSI), Darmstadt, Germany, <sup>8</sup>University of California at Davis, Davis, USA, <sup>9</sup>Joint Institute for Nuclear

Research, Dubna, Russia, <sup>10</sup>Fachbereich Physik der Universität, Frankfurt, Germany, <sup>11</sup>University of California at Los Angeles, Los Angeles, USA, <sup>12</sup>Fachbereich Physik der Universität, Marburg, Germany, <sup>13</sup>Max-Planck-Institut für Physik, Munich, Germany, <sup>14</sup>Institute for Nuclear Studies, Warsaw, Poland, <sup>15</sup>Institute for Experimental Physics, University of Warsaw, Warsaw, Poland, <sup>16</sup>Nuclear Physics Laboratory, University of Washington, Seattle, WA, USA, <sup>17</sup>Yale University, New Haven, CT, USA, <sup>18</sup>Rudjer Boskovic Institute, Zagreb, Croatia.

<sup>†</sup>Alexander von Humboldt Foundation (Lynen) Fellow. <sup>\*</sup>Alexander von Humboldt Foundation U.S. Senior Scientist Award Recipient.

<sup>§</sup>present address: Brookhaven National Laboratory, Upton, N.Y. <sup>#</sup>present address: Physikalisches Institut, Universität Heidelberg, Germany.

**Abstract.** Using the NA49 main TPC, the central production of  $(\Xi + \bar{\Xi})$  hyperons has been measured in CERN SPS Pb on Pb collisions at 158 GeV/c. The preliminary  $(\Xi + \bar{\Xi})/(\Lambda + \bar{\Lambda})$  ratio, studied at  $2.0 < y < 2.6$  and  $1 < p_T < 3$  GeV/c, equals  $\sim 13 \pm 3$  % (systematic error only). It is compatible, within errors, with the previously obtained ratios for central S+S [1], S+W [2], and S+Au [3] collisions. The fit to the transverse momentum distribution resulted in an inverse slope parameter  $T$  of 297 MeV. At this level of statistics we do not see any noticeable enhancement of hyperon production with the increased volume (and, possibly, degree of equilibration) of the system from S+S to Pb+Pb. This result is unexpected and counterintuitive, and should be further investigated. If confirmed, it will have a significant impact on our understanding of mechanisms leading to the enhanced strangeness production in heavy ion collisions.

## 1. Introduction

Measurements of doubly strange baryons and antibaryons in high energy heavy ion collisions allow us to probe into the dynamics of hot and dense nuclear matter [4], [5], [6]. In particular, heavy hyperons ( $\Xi$ ,  $\Omega$ ) appear to be important since, due to their large mass, they are likely to be produced in the early stages of the collisions when the nuclear density is the highest, and, therefore new phenomena (e.g., phase transitions [7]), are likely to occur. So far only a few data on the production of these particles in heavy ion reactions exist, and their relation to the global characteristics of the events is not well established. Since the consensus of the field is that no one measurable quantity can unambiguously signal the occurrence of a new phenomenon, it is necessary to study many global observables simultaneously and use the combined information to investigate and isolate possibly new physics. The NA49 experiment provides a very good match to these requirements. The multi-strange hyperon production

measurements are complemented by the detailed global analysis of the collisions [8], and eventually may lead to definite constraints on the reaction dynamics.

This paper presents results obtained by the NA49 experiment on the production of  $(\Xi + \bar{\Xi})$  at the CERN SPS based on a study of the decays of  $\Xi \rightarrow \Lambda + \pi^-$  (where  $\Lambda \rightarrow p + \pi^-$ ) and  $\bar{\Xi} \rightarrow \bar{\Lambda} + \pi^+$  (where  $\bar{\Lambda} \rightarrow \bar{p} + \pi^+$ ) from about 50,000 central Pb+Pb events. The measurements were done without magnetic field.

The idea of strangeness 2 baryon measurements in the absence of the magnetic field, was in principle, already used before in the UA5 analysis of  $p\bar{p}$  collisions at  $\sqrt{S}=540$  GeV/c [9]. But, because of totally different method of detection (streamer chamber vs TPC) and significantly lighter environment (track multiplicity lower by one order of magnitude), the procedure developed by UA5 experiment was not applicable for the heavy ion collision case.

The outline of the paper is as follows: In sect.2 the NA49 detector and the data analysis procedure are described. In sect.3 the results are presented and discussed, and a comparison with existing data is made. Conclusions are drawn in sect.4

## 2. Experimental Procedure

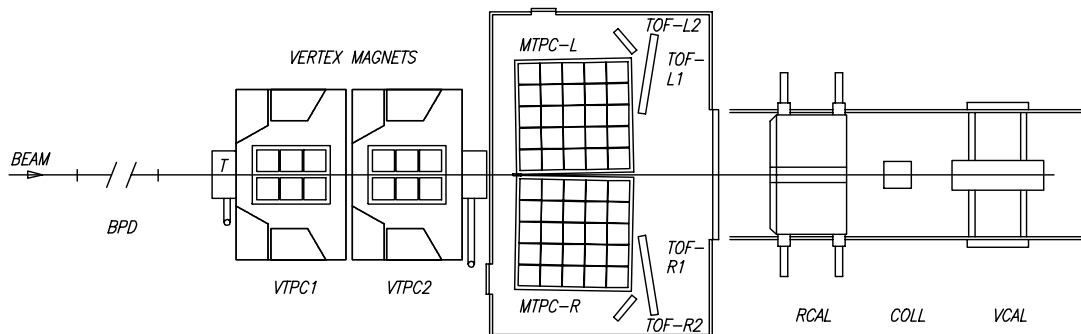


**Figure 1.** The NA49 experimental set-up.

The detailed description of the apparatus can be found in [8] and references therein. Fig.1 shows a schematic layout of the NA49 detector. It consists of four large Time Projection Chambers (TPC) as tracking devices, a Time of Flight (TOF) system, and a set of calorimeters for transverse and forward energy flow measurements. For this analysis the NA49 experiment was run in a special configuration with the target removed from its standard position (see Fig.1) and mounted directly upstream from the MTPCs (see Fig.2), which are situated outside the magnetic field on either side of

the beam. Two vertex TPC's (VTPC1 and VTPC2 in Fig.1), usually operating in the magnetic field, did not participate in this data taking. Using the forward energy distribution, a centrality cut was made to select on-line only the most central events ( $\sim 6\%$  of the total inelastic cross section).

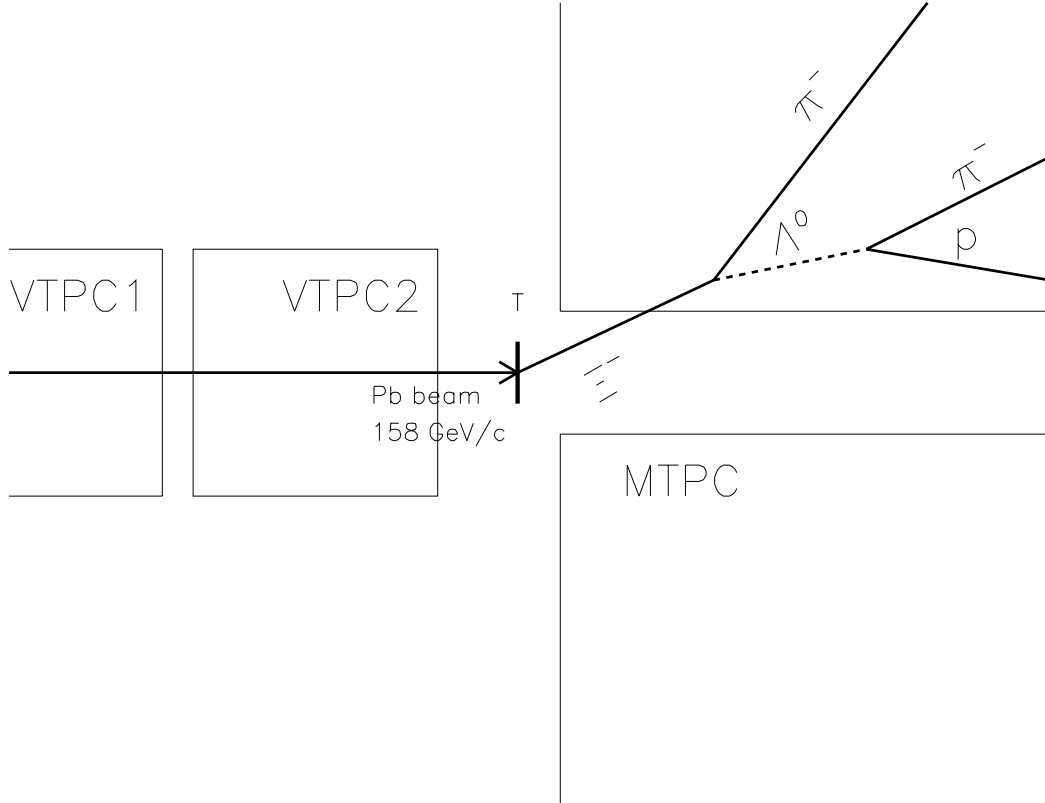


**Figure 2.** The NA49 experimental set-up in the configuration for the  $\Xi$  run.

Data were obtained during two different runs. The first was in October-November of 1995 with the trigger corresponding to 5 % of  $\sigma_{inel}^{tot}$  (18,870 events). The second was in November 1996 with more relaxed trigger of 7 % of  $\sigma_{inel}^{tot}$  (240,000 events collected, out of which 29,249 were used for this analysis). Data from 1995 correspond to the impact parameter  $b < 3.3$  fm, whereas 1996 data to  $b < 4$  fm.

The cascade decay

$$\Xi \rightarrow \Lambda + \pi^- \quad (\text{where } \Lambda \rightarrow p + \pi^-)$$

has a very characteristic topology: a  $V^0$  is “seen” to point back to a charged decay

vertex (“kink”) rather than to the primary event vertex. An example of such a cascade decay is sketched in Fig.2.

At this stage of the analysis, our sample of cascade particles includes also  $\Xi$ ,  $\Omega$  and  $\bar{\Omega}$ , since their topologies are identical (for the  $\Omega$  and  $\bar{\Omega}$ , a  $K$ , instead of a  $\pi$ , is produced in the first vertex). Likewise  $\Lambda$  indicates the sum of  $\Lambda$ ,  $\bar{\Lambda}$ ,  $\Sigma^0$  and  $\bar{\Sigma}^0$ . So far, the  $dE/dx$  information available from the TPCs which can be used for particle ID, is not implemented yet. It is, however, reasonable to assume that the population of  $\Xi$  vastly dominates the rest of the multi-strange hyperons in the data sample. In the configuration with no magnetic field, the reconstruction of the  $V^0$ -type vertices is done the conventional way (by combining track pairs), but with straight, not curved, tracks [10]. The sample of  $V$ 's included decays of  $K_L$ ,  $K_S$ ,  $\Lambda$ , and  $\bar{\Lambda}$ , and photon conversions in the chamber gas. Photon conversions were eliminated by demanding the  $V^0$  opening angle to be greater than 2 degrees. To separate  $K_L$  decays, we used the fact that  $K_S$ ,  $\Lambda$ , and  $\bar{\Lambda}$  all decay into two particles and, therefore, the primary and two secondaries (decay products) should be coplanar. In the absence of momentum measurements on the secondary tracks, each coplanar  $V$  could be either  $K_S$ ,  $\Lambda$  or  $\bar{\Lambda}$ . The separation of  $K^0$  from the  $\Lambda / \bar{\Lambda}$  is done by placing cuts on the angles between the parent and daughter particles. In  $\Lambda / \bar{\Lambda}$  decays the opening angle of the proton/antiproton cannot exceed a certain value, whereas the  $K^0$  decay is symmetric. The background was found to be combinatoric and dependant on the set of cuts. For the details see our paper on neutral strange particle production [11]. The next step of the analysis is totally new and therefore requires much more explanation. For each  $\Lambda$  candidate (= pair of two tracks which could be the products of  $\Lambda$  decay) the search was continued to find the second, matching “visible” cascade decay product. The match criterion is coplanarity of the visible track,  $\Lambda$  decay vertex, and interaction vertex. At first, roughly coplanar candidates were selected (triplets of tracks) which, together with the preliminary values of both vertex positions, served as start parameters (“seed” values) for the MINUIT fit. The preliminary values of the vertex coordinates were estimated in the following way:

for the  $V^0$  vertex - from the distance of the closest approach for the  $\Lambda$  decay products,  
 for the  $\Xi$  (“kink”) vertex - from the intersection of  $\pi$  trajectory with the  $\Lambda$  decay plane.  
 MINUIT refitted these values using the coplanarity constraint. Both vertices and all three trajectories were fitted simultaneously (10 parameter fit), allowing for the adjustment of final vertex coordinates (within the point positions resolution) to satisfy the coplanarity assumption. In this procedure all available experimental information ( $x$ ,  $y$ , and  $z$  of all measured points along the tracks) was used simultaneously. The coplanarity constraint used in fitting routines appeared to be extremely powerful in eliminating the vast majority of the combinatorial background.

The momentum of the parent and daughter particles can be inferred in each vertex

from the decay angles if one assumes their masses. This was done by solving the energy/momentum conservation equation in each vertex, separately. Plugging the  $\Lambda$  momentum, calculated at the  $V^0$  vertex, into the energy/momentum conservation equations for the “kink” vertex, allowed us to calculate the  $\Xi$  mass rather than to assume it.

### 3. Results

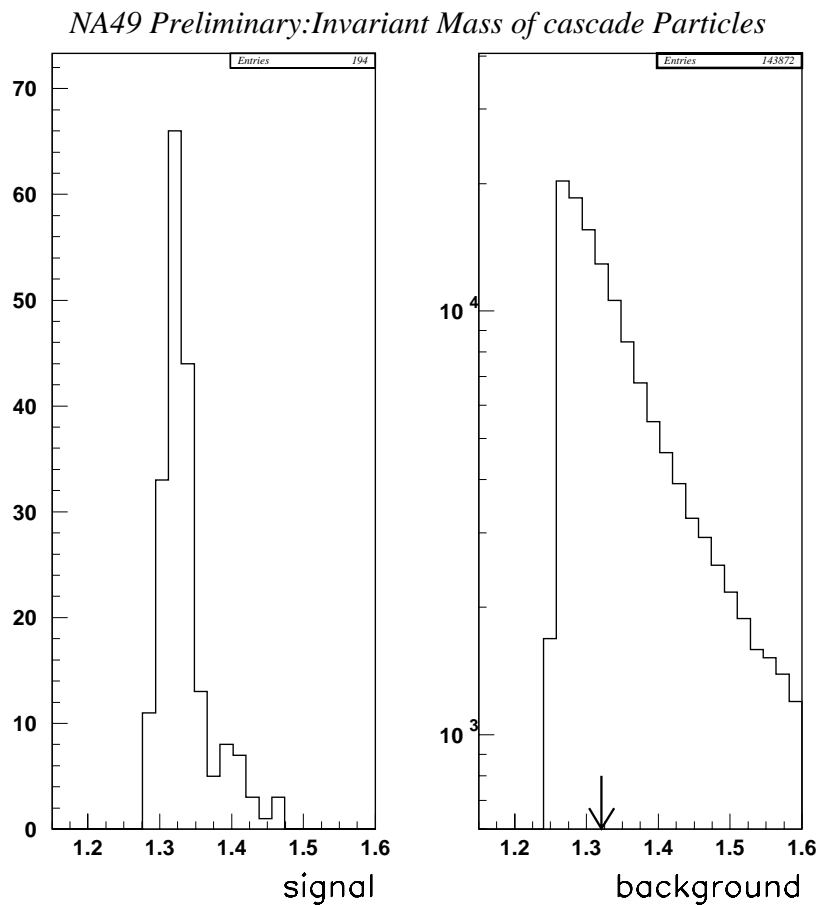


**Figure 3.** The  $\Xi$  invariant mass spectrum (left), and the background distribution (right). See text for details.

The entire procedure was tested on 20,000 simulated events. The set of cuts was applied to remove the combinatorial background. Major ones, besides the already discussed noncoplanarity, include the distance of closest approach between  $\Lambda$  decay

products, distances of  $\Xi$  and  $V^0$  vertices from the interaction vertex, minimum number of hits on tracks to be considered in the analysis, impact parameters of  $\Xi$  decay products, etc. After cuts, the background was reduced to 0.017% of its original value, whereas 5.4% of the signal (=number of  $\Xi$  in the simulated events) was still preserved. Final ratio of (background+signal)/signal amounted to  $\sim 1.3$  (ratio=1 would correspond to the total elimination of the background).

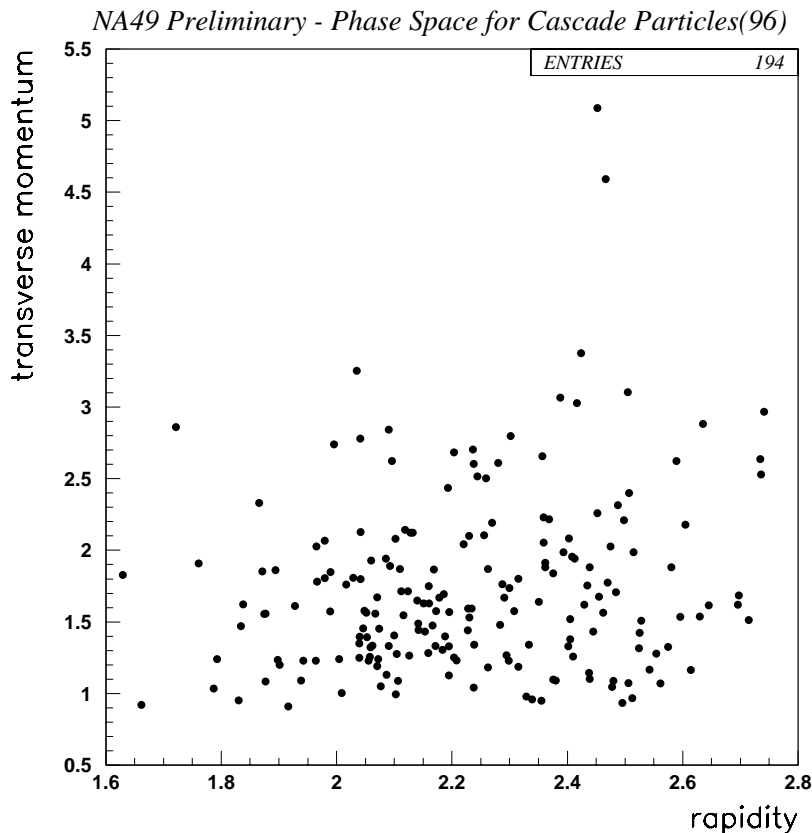


**Figure 4.** The rapidity vs transverse momentum distribution for  $\Xi$  particles from '96 run.

Tighter cuts, to reduce background to the  $\sim 7\%$  level ( $(B+S)/S$  ratio of 1.07), were successfully implemented into the analysis of the simulated events. However, they were found to be impractical at the present level of available statistics for the experimental data.

The invariant-mass plot for  $\Xi$  particles from the '96 data ( $\sim 30,000$  events) is presented in Fig.3. The right panel shows the background (all relevant combinations of



NA49 preliminary

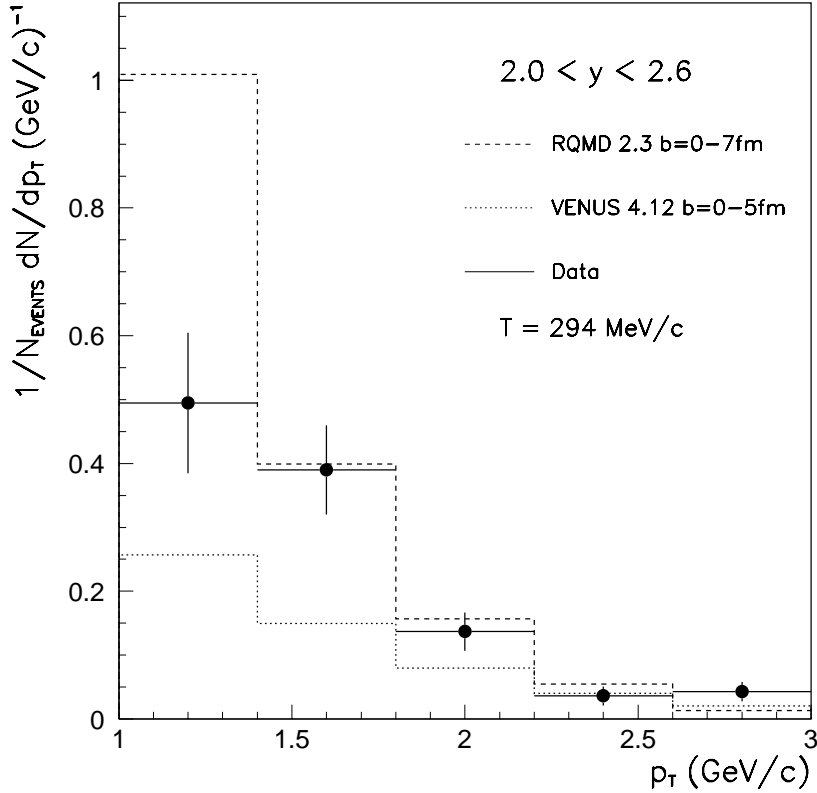


**Figure 5.** The transverse momentum spectrum of  $\Xi$  particles in the rapidity bin  $2 < y < 2.6$ .

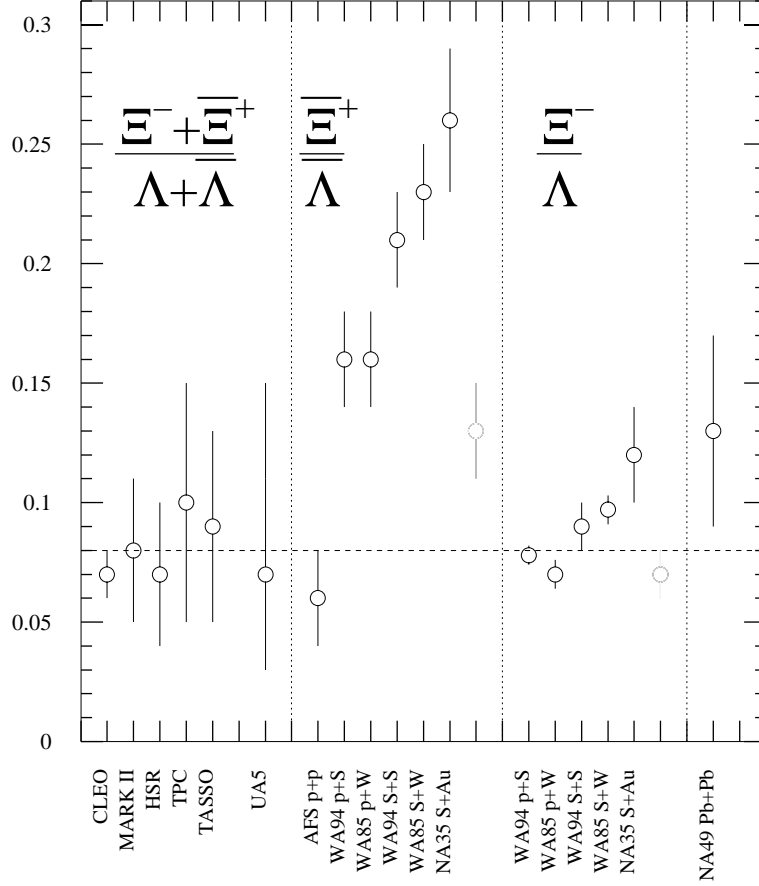
tracks) and the left shows the  $\Xi$  signal, extracted with the above procedure. Applied cuts selected a cascade particle sample with very little background. A clean peak is seen at a mass of 1.327 GeV, which is very close to value of Particle Data Book (1.321 GeV). For reference, the small arrow marks this value on the background distribution (right panel).

Figure 4 shows the  $p_T$  vs  $y$  plot for these data.

Equivalent plots for the '95 run ( $\sim 20,000$  events) look very similar.

To obtain a statistically meaningful  $dN/dp_T$  distribution data samples from '95 and '96 runs were combined and the phase space was restricted to one rapidity bin:  $2.0 < y < 2.6$ . The range of  $p_T$  covers 1-3 GeV/c.

The reconstruction efficiency was estimated by either using fully simulated Pb+Pb events or by embedding simulated decays into raw events. Figure 5 shows the



**Figure 6.** The  $\Xi/\Lambda$  and  $\Xi/\bar{\Lambda}$  ratios for different experiments at CERN SPS energies.

preliminary acceptance and efficiency corrected spectrum of  $dN/dp_T$ . The inverse slope parameter, 294 MeV, aligns well with the systematic trend of increasing  $T$  with particle mass observed earlier [12]. Venus 4.12 and RQMD 2.3 model predictions are marked in Fig.5 for comparison. Both models failed to reproduce the data. The discrepancy is particularly significant in the low  $p_T$  bins.

The integrated and to the full  $p_T$  range extrapolated value of the  $dN/dp_T$  (from Fig.5) was compared to the same integral for  $(\Lambda + \bar{\Lambda})$  in the same rapidity acceptance [12]. The ratio  $(\Xi + \bar{\Xi})/(\Lambda + \bar{\Lambda}) \cong 13 \pm 3\%$  (systematic error only), agrees with values for the lighter systems S+S, S+W and S+Au at 200 GeV/c - see Fig.6.

One of the strongest points of the NA49 analysis lies in the fact that the experiment provides the capability of performing independent measurements of physics

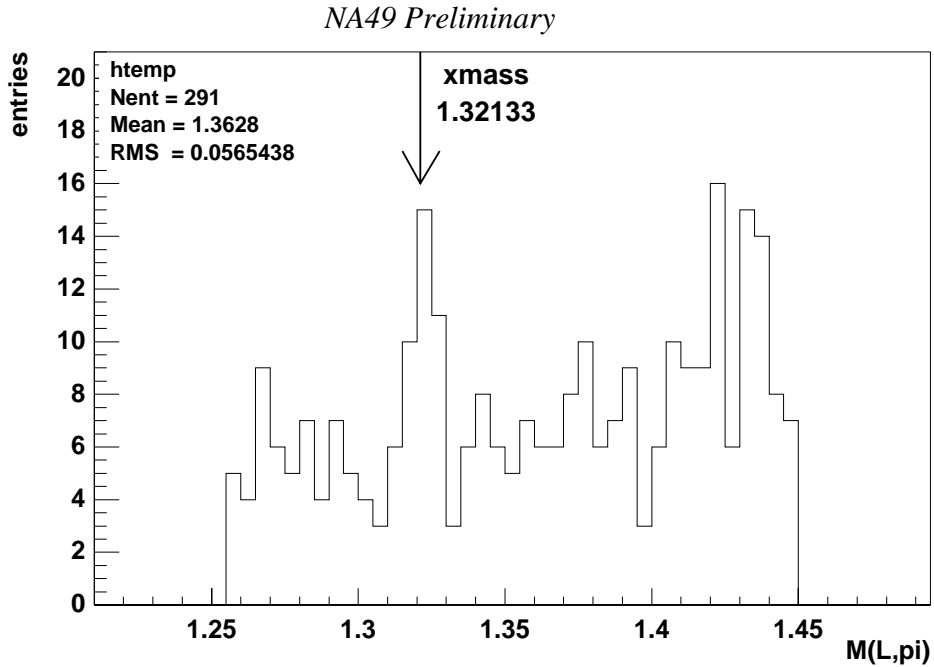


**Figure 7.** The inv. mass plot of  $\Xi$  obtained with VTPC2 before background subtraction.

observables in more than one way. Such a redundancy is particularly important in the case of rare and/or exotic species. In case of multi-strange hyperons, besides the already described analysis without magnetic field, the  $\Xi$ 's and  $\Omega$ 's are being studied in the standard way with a magnetic field and direct momentum measurements in the vertex TPC (VTPC2). Analysis is still in a very early stage; however, the preliminary plot of the invariant-mass spectrum shows a distinct maximum (Fig.7) at the correct value for the cascade particle. Rapidity coverage of VTPC2 ( $2.5 < y < 4.5$ ) is complementary to that from the MTPC, so that both detectors together cover entirely the available phase space for  $\Xi/\Omega$  production.

#### 4. Summary

The new method of measuring and analyzing multi-strange hyperons in the absence of a magnetic field was proposed and implemented. This method makes use of the easier/high-accuracy (straight line) tracking in the large MTPC volumes in the absence of  $\mathbf{E} \otimes \mathbf{B}$  distortions. A very high degree of background rejection based on a

coplanarity constraint was demonstrated. This allowed us to avoid the standard statistical approach with deconvolution of signal and background peaks in the invariant-mass distribution and led to the direct rapidity and transverse momentum spectra. It provides a tremendous advantage in the very high multiplicity environment where the standard analysis suffers from low efficiency.

On the physics side: 278  $\Xi$  and  $\bar{\Xi}$  ( $+ \Omega$  and  $\bar{\Omega}$ ) particles were measured in 48,119 central Pb+Pb events for  $2 < y < 2.6$  and  $1 < p_T < 3$  GeV/c. The ratio  $(\Xi + \bar{\Xi})/(\Lambda + \bar{\Lambda})$  was estimated to be  $\sim 13 \pm 3\%$ , which is consistent with the equivalent ratios measured in lighter systems (S+S, S+Pb and S+Au).

Increased statistics will extend the rapidity coverage and permit a more detailed study of  $\Xi$  production in central Pb+Pb collisions. Application of more stringent cuts (already tested on MC events) will lead to almost total background rejection. Over 240,000 events with the MTPC, and about 2 million with the VTPC2, were collected. The full sets are presently being analyzed.

Separation of  $\Xi/\bar{\Xi}$  and  $\Omega/\bar{\Omega}$  will be done by a kinematic fit.

If, with further analysis, the results remain unchanged, that will mean that this unknown, new and very efficient mechanism of strangeness production which we observe in nucleus-nucleus collisions at CERN energies [13], [14], is independent of the volume of the interacting system and/or on the degree of equilibration. A similar observation was already made in regard to kaon production (NA49 and NA44 experiments) [15], where it was observed that the ratio of  $K^0$  (NA49) and  $K^+$ ,  $K^-$  (NA44) yields to pion yields in Pb+Pb were very similar to those observed in S+Au. This is an astonishing result and may lead to significant changes in our understanding of these aspects of the collision dynamics which are related to the degree and nature of flavour equilibration, and/or are responsible for the strangeness production mechanisms in heavy ion interactions.

## References.

- [1] Kinson J B et al., 1995 *Nucl. Phys.* **A590** 317c and references therein
- [2] Abatzis S et al., 1991 *Phys. Lett.* **270B** 123, 1992 *Nucl. Phys.* **A544** 321c, 1994 *Nucl. Phys.* **A566** 225c
- [3] Retek W and the NA35 Coll. 1997 in this proceedings
- [4] Rafelski J and Muller B 1982 *Phys. Rev. Lett.* **48** 1066, 1986 *Phys. Rev. Lett.* **56** 2334
- [5] Koch P, Muller B and Rafelski J 1986 *Phys.Rep.* **142** 167
- [6] Ellis J and Heinz U 1989 *Phys. Lett.* **233B** 223
- [7] Rafelski J 1991 *Phys. Lett.* **262B** 333
- [8] Jones P and the NA49 Coll. 1996 *Nucl. Phys.* **A610** 188c
- [9] Alner G J et al., 1985 *Phys. Lett.* **151B** 309
- [10] Alpgard K et al., 1982 *Phys. Lett.* **115B** 65
- [11] Margetis S and the NA49 Coll. 1996 *Heavy Ion Phys.* **4** 63

- [12] Bormann C and the NA49 Coll. 1997 in this proceedings
- [13] Proceedings of Strangeness'95 Conf., 1995 AIP Press, 340
- [14] Proceedings of Strangeness'96 Conf., 1996 Heavy Ion Physics **4**
- [15] Odyniec G 1996 ICHEP'96, World Scientific, Vol.1,964.

**Acknowledgement.**

This work was supported by the U.S. Department of Energy, the Bundesministerium für Bildung und Forschung, Germany, the Research Secretariat of the University of Athens, the Polish State Committee for Scientific Research, the Polish-German Foundation, the Hungarian Scientific Research Fundation and EPSRC, U.K.